

Supplementary Information

Accumulated photogenerated holes in Type-II ZnSe/CdS nanotetrapods for efficient photocatalytic hydrogen evolution

*Zhi-Kai Qin[#], Li-Lei Shen[#], Shuo Yan, Jingui Wang, and Yu-Ji Gao**

School of Chemistry and Chemical Engineering, Faculty of Chemistry and Pharmacy,
Qilu University of Technology (Shandong Academy of Science), Jinan, Shandong
250353, P. R. China

*Corresponding authors. Email address: yjgao@qlu.edu.cn (Y.-J. Gao).

Characterization

Powder X-ray diffraction (XRD) patterns were obtained by using Bruker D8-ADVANCE (Bruker Corp, Billerica, MA, USA) with Cu-K α radiation. X-ray photoelectron spectroscopy (XPS) were recorded on an ESCALAB 250 spectrophotometer (Thermo Fisher Scientific Corp, Waltham, MA, USA) with Al-K α radiation. The binding energy scale was calibrated using the C1s peak at 284.60 eV. Elemental analysis data were obtained from Inductively coupled plasma-mass spectrometry (ICP-MS, 7890A+5975C, Agilent, USA). TEM images were obtained from JEM 2100 (JEOL Co. Ltd., Tokyo, Japan). UV-vis absorption spectra were recorded on a Shimadzu UV-2600PC spectrophotometer (Shimadzu Corp, Kyoto, Japan). Photoluminescence (PL) spectra were obtained by Hitachi (F-4600) spectrophotometer (Hitachi High-Tech Corp., Tokyo, Japan). The content of H₂ in the product was determined by gas chromatography (GC, GC-2014, Shimadzu Corp., Kyoto, Japan), and using Ar as the carrier gas with a molecular sieve column (5 Å; 30 m \times 0.53 mm) and a thermal conductivity detector. The photoelectrochemical measurement was carried out on an electrochemical workstation (CHI 660B, Chinstruments, Shanghai, China). High angle annular dark field (HAADF)-scanning transmission electron microscopy (STEM) images and energy-dispersive X-ray spectroscopy (EDS) maps were acquired using an aberration-corrected JEM-ARM300F (JEOL Co. Ltd., Tokyo, Japan) operated at 80 kV. The steady-state surface photovoltage (SPV) measurement system includes computer, lock-in amplifier, monochromatic light and photovoltaic cell. The monochromatic light was provided by Xe lamp (300 W) and a double-prism monochromator. Femtosecond transient absorption (TA) spectroscopy was measured with pump pulse at 360 nm and probing with white light, the 360 nm pulse was produced by second-harmonic generation of the fundamental output of the Ti:sapphire regenerative amplifier (Coherent Legend Elite, 4 mJ, 25 fs, 1KHz).

Apparent Quantum Yield (AQY)

The apparent quantum yield (AQY) of ZnSe/CdS NTPs was measured under the monochromatic LED light sources ($\lambda = 460 \text{ nm}$, 100 mW cm^{-2}) with the irradiation area of $2.0 \times 1.2 \text{ cm}^2$. $344.8 \text{ }\mu\text{mol}$ of H_2 was produced under 1 h irradiation for the ZnSe/CdS NTPs. The AQY was calculated as 20.8 % according to the following equation (S1):

$$AQY = \frac{N_e}{N_p} \times 100\% = \frac{10^9 \times v \times N_A \times K \times h \times c}{I \times A \times \lambda} \times 100\% \quad (S1)$$

Where N_e is number of reacted electrons; N_p is number of incident photons; v is reaction rate (mol s^{-1}); N_A is the Avogadro constant ($6.022 \times 10^{23} \text{ mol}^{-1}$); K is number of electrons transferred ($K=2$ for photocatalytic H_2 evolution); h is the Plank constant ($6.626 \times 10^{-34} \text{ J s}$); A is the irradiation area (m^2); I is the monochromatic light intensity (W m^{-2}); λ is the wavelength of the monochromatic light (nm); c is the speed of light ($3 \times 10^8 \text{ m s}^{-1}$).

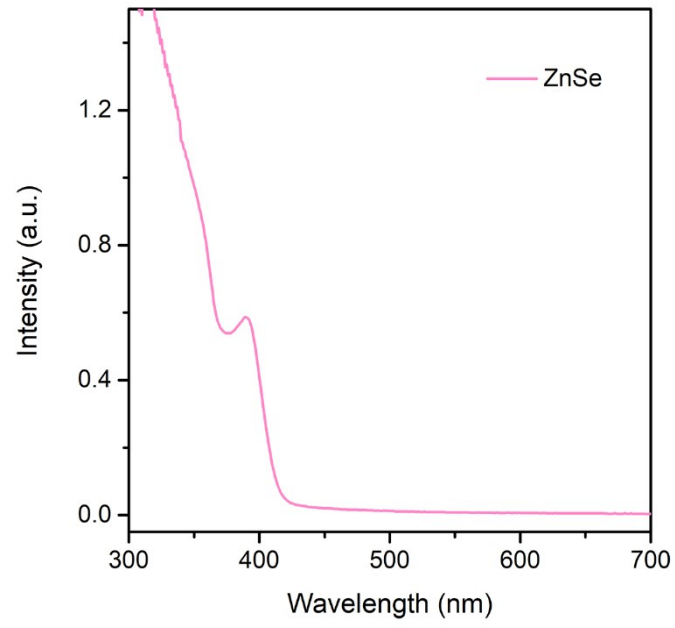


Fig. S1 The UV-vis absorption spectrum of ZnSe QDs.

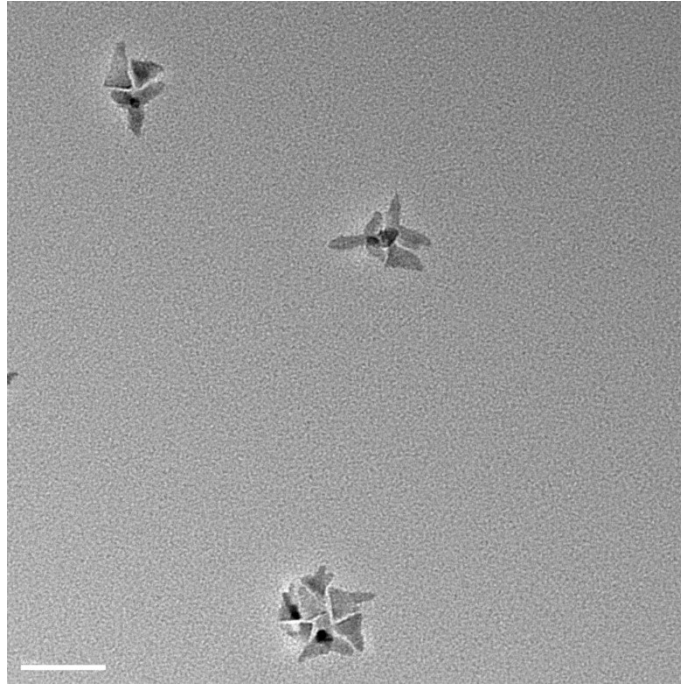


Fig. S2 The TEM images of thick ZnSe/CdS NTPs. Scale bar: 50 nm.

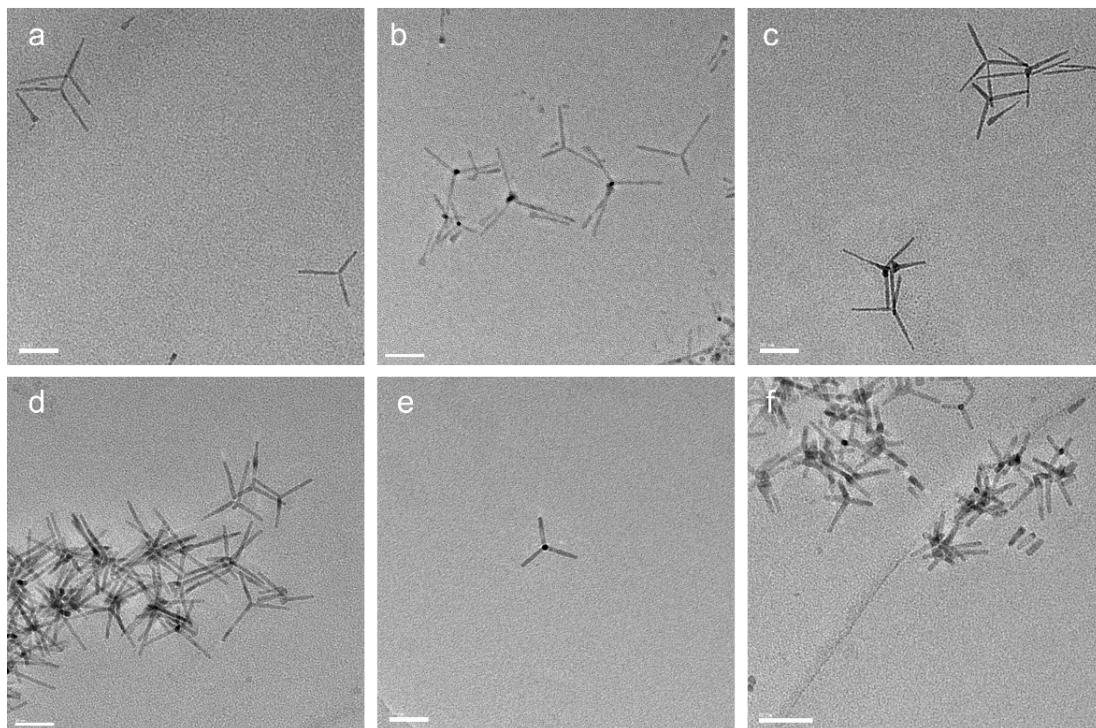


Fig. S3 The TEM images of (a) CdS NTPs and (b-f) ZnSe_x/CdS NTPs with different amounts of ZnSe seed during the synthetic process. The amount of ZnSe seed from b to f is 1.25×10^{-9} mol, 2.5×10^{-9} mol, 5.0×10^{-9} mol, 7.5×10^{-9} mol, and 10.0×10^{-9} mol, respectively. Scale bar: 50 nm.

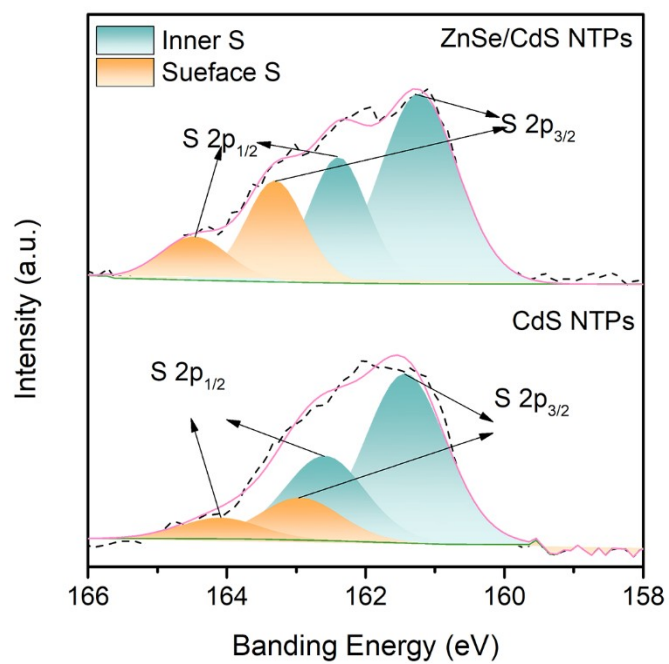


Fig. S4 High-resolution XPS analysis of S 2p spectra for CdS and ZnSe/CdS NTPs.

Table S1 Inductively coupled plasma-mass spectrometry (ICP-MS) results of ZnSe/CdS NTPs.

Elements	Dilution Multiple^[a]	Raw data (mg/L)	Element content (mg/g)	Element content (wt%)
Cd	50	7.49	394.0	39.4%
S	50	2.37	124.4	12.4%
Se	1	7.28	7.66	0.8%
Zn	1	2.06	2.17	0.2%

[a]: The solution was diluted by 50 times for the concentration test of Cd and S, while Zn and Se were measured at the original solution.

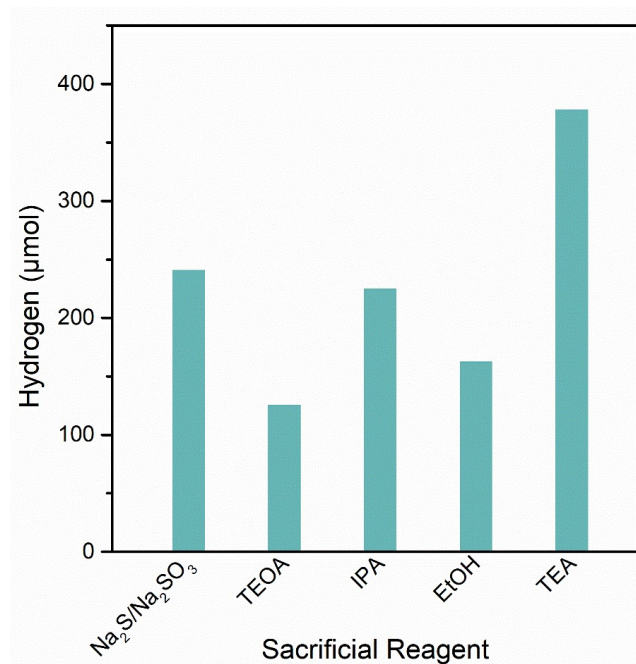


Fig. S5 Photocatalytic H₂ evolution for ZnSe/CdS NTPs under different sacrificial reagents within 4 h irradiation. The ZnSe/CdS NTPs would produce H₂ efficiently under various sacrificial reagents. While the TEA gives the highest hydrogen production amount. Therefore, TEA serves as the sacrificial reagents throughout the entire reaction process.

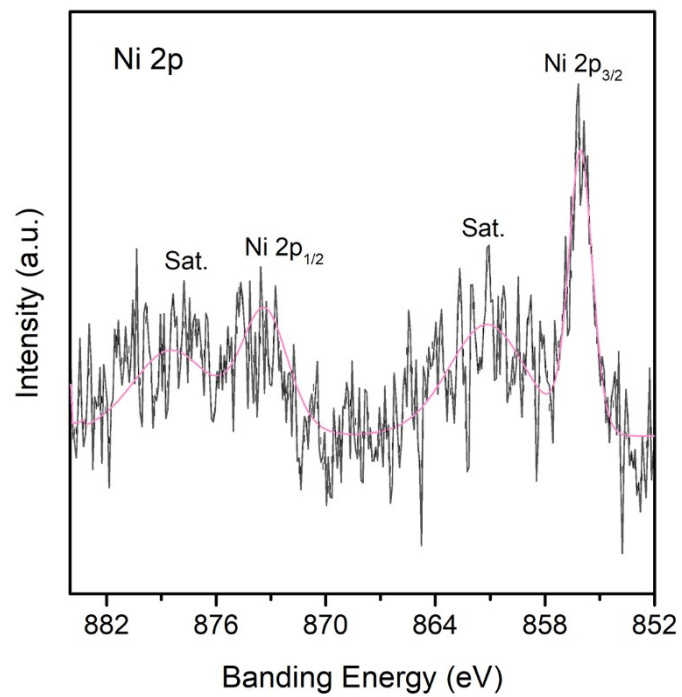


Fig. S6 High-resolution XPS analysis of Ni 2p spectra for ZnSe/CdS NTPs.

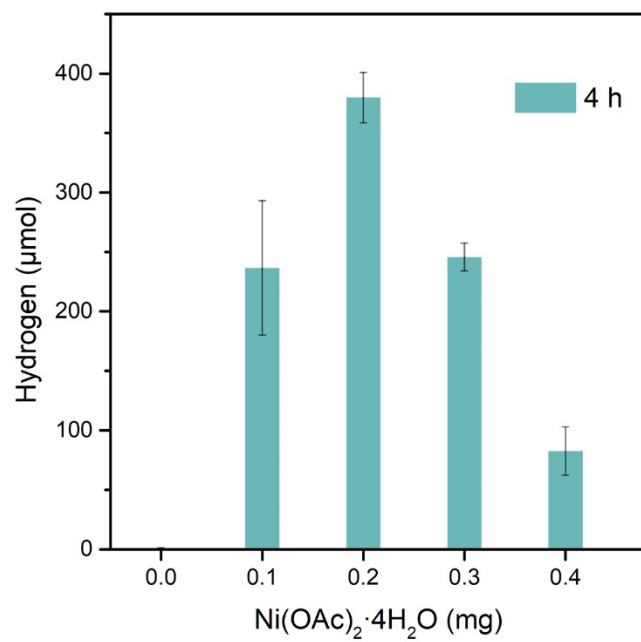


Fig. S7 Comparison of H₂ evolution for ZnSe/CdS NTPs under different amount of Ni(CH₃COO)₂·4·H₂O. Error bars represent the mean ± s.d. of multiple independent experiments.

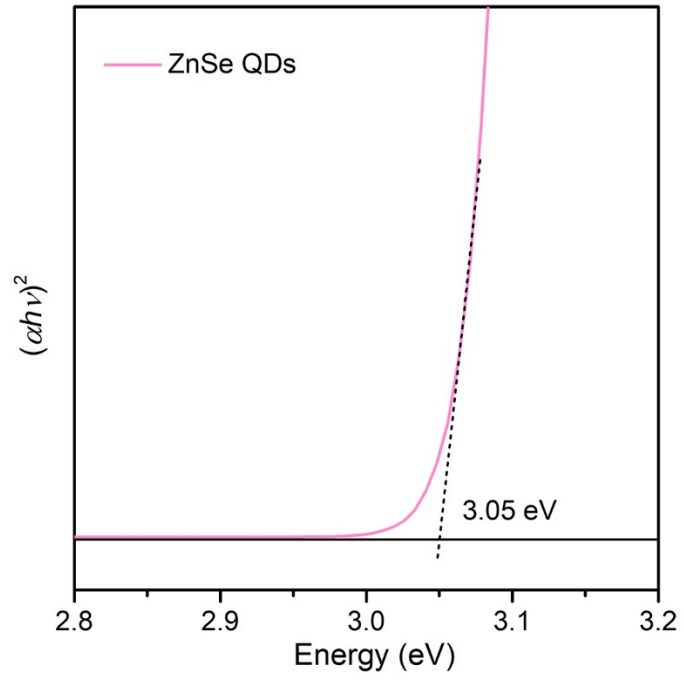


Fig. S8 Tauc plots of ZnSe QDs.

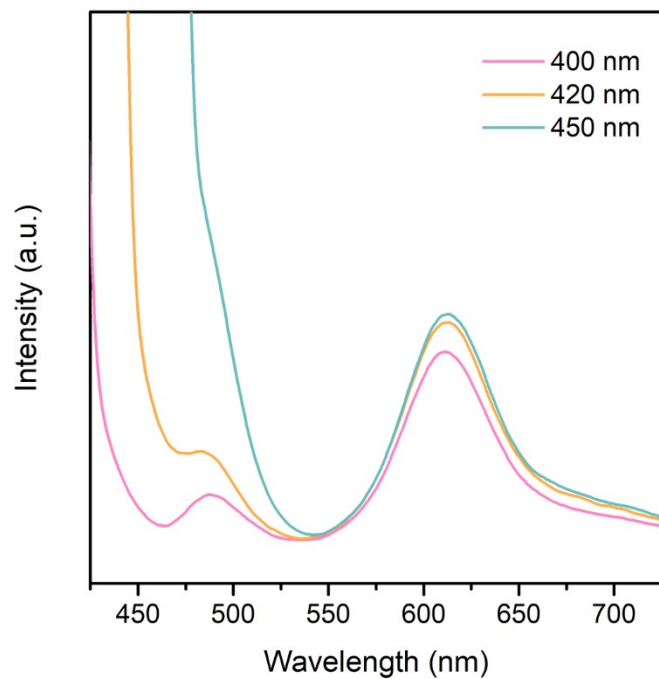


Fig. S9 Photoluminescence (PL) spectra of ZnSe/CdS NTPs with different excitation wavelength.

Table S2 Comparison of photocatalytic H₂ evolution with reported colloidal nanocrystals based systems.

Photocatalyst	Co-catalyst	Light Source	Donor	Rate of H ₂ Evolution ^[a] ($\mu\text{mol h}^{-1} \text{mg}^{-1}$)	TON	AQY (%)	Time (h)	Refer
Ni-CdS NRs	None	447 nm	EtOH	63	None	53	4	[1]
CdSe/CdS	None	>420 nm	TEOA	16.03	None	None	4	[2]
CdS QDs	Co ²⁺	>420 nm	Na ₂ SO ₃	----	29000	None	88	[3]
CdS QDs	Ni ²⁺	>400 nm	Glycerol	74.6	38405	None	20	[4]
CdS QDs	Cobaloxime	>420 nm	TEOA	2.3 ^[b]	171	None	15	[5]
CdS QDs	None	>400 nm	N ₂ H ₄ ·H ₂ O	33	14.16	None	4	[6]
NiS ₂ -C/CdS NSs	None	>420 nm	Na ₂ S and Na ₂ SO ₃	92.19	None	None	5	[7]
Pt _{SA+C} /CdS	None	>420 nm	Lactic acid	80.4	58818	None	6	[8]
CdS@MoS ₂ /Ti ₃ C ₂	None	420 nm	Lactic acid	14.88	None	None	78	[9]
CdS/ZnS-ReS ₂	None	≥420 nm	Na ₂ S and Na ₂ SO ₃	10.72	None	1.7	2	[10]
CdS/TiO ₂	None	300 W Xe lamp	Na ₂ S and Na ₂ SO ₃	21.4	None	None	4	[11]
NiS/CdS NPs	None	≥420 nm	Lactic acid	7.49	None	None	16	[12]
CoP QDs/CdS NRs	None	>400 nm	Lactic acid	104.95	None	32.16	12	[13]
Co ₃ N/CdS	None	>420 nm	Na ₂ S and Na ₂ SO ₃	137.33	None	14.9	48	[14]
CdS	None	≥420 nm	Na ₂ S and Na ₂ SO ₃	9.58	None	4.12	15	[15]
CdS/Pt/Mo ₂ C	None	>400 nm	Na ₂ S and Na ₂ SO ₃	1.83	None	9.39	20	[16]
ZnSe/CdS NTPs	Ni ²⁺	460 nm	TEA	142.89	1.71×10^8	20.8	100	This work

[a]: All units are converted to $\mu\text{mol h}^{-1} \text{mg}^{-1}$ according to the results provided in the articles.

[b]: The data is calculated according to the data in the article.

References

- [1] T. Simon, N. Bouchonville, M. J. Berr, A. Vaneski, A. Adrović, D. Volbers, R. Wyrwich, M. Döblinger, A. S. Susha, A. L. Rogach, F. Jäckel, J. K. Stolarczyk and J. Feldmann, *Nat. Mater.*, 2014, **13**, 1013.
- [2] R. Lv, K. Ye, W. Zhang, H. Chen, R. Zhao, H. Wu and M. Chen, *Colloid Surf. A-Physicochem. Eng. Asp.*, 2024, **684**, 133143.
- [3] C. M. Chang, K. L. Orchard, B. C. M. Martindale and E. Reisner, *J. Mater. Chem. A*, 2016, **4**, 2856.
- [4] J.-J. Wang, Z.-J. Li, X.-B. Li, X.-B. Fan, Q.-Y. Meng, S. Yu, C.-B. Li, J.-X. Li, C.-H. Tung and L.-Z. Wu, *ChemSusChem*, 2014, **7**, 1468.
- [5] F. Wen, J. Yang, X. Zong, B. Ma, D. Wang and C. Li, *J. Catal.*, 2011, **281**, 318.
- [6] M. K. Jana, U. Gupta and C. N. R. Rao, *Dalton Trans.*, 2016, **45**, 15137.
- [7] B. Yu, X. Chen, C. Huang and W. Yao, *Appl. Surf. Sci.*, 2022, **592**, 153259.
- [8] J. Zhang, Y. Pan, D. Feng, L. Cui, S. Zhao, J. Hu, S. Wang and Y. Qin, *Adv. Mater.*, 2023, **35**, 2300902.
- [9] C. Wu, W. Huang, H. Liu, K. Lv and Q. Li, *Appl. Catal. B Environ.*, 2023, **330**, 122653.
- [10] N. Su, Y. Bai, Z. Shi, J. Li, Y. Xu, D. Li, B. Li, L. Ye and Y. He, *ACS Omega*, 2023, **8**, 6059.
- [11] V. Navakoteswara Rao, P. Kedhareswara Sairam, M.-D. Kim, M. Rezakazemi, T. M. Aminabhavi, C. W. Ahn and J.-M. Yang, *Journal of Environmental Management*, 2023, **340**, 117895.
- [12] K. Zhang, Z. Mou, S. Cao, S. Wu, X. Xu and C. Li, *Int. J. Hydrog. Energy*, 2022, **47**, 12605.
- [13] Q. Sun, Z. Yu, R. Jiang, Y. Hou, L. Sun, L. Qian, F. Li, M. Li, Q. Ran and H. Zhang, *Nanoscale*, 2020, **12**, 19203.
- [14] H. Zhen, D. Jiang, Z. Sun, R. Muhammad Irfan, L. Zhang and P. Du, *Catal. Sci. Technol.*, 2017, **7**, 1515.
- [15] S. Cui, R. Ao, Z. Lin and M. Ding, *Int. J. Hydrog. Energy*, 2024, **51**, 848.
- [16] X. Jing, X. Peng, Y. Cao, W. Wang and S. Wang, *RSC Adv.*, 2018, **8**, 33993.